

A comparison of orbital interactions in the additions of phosphonyl and acyl radicals to double bonds†

Elizabeth H. Krenske*‡^{a,b} and Carl H. Schiesser^{a,c,d}

Received 21st September 2007, Accepted 11th December 2007

First published as an Advance Article on the web 14th January 2008

DOI: 10.1039/b714597g

Calculation of the barriers for addition of the $\text{H}_2\text{P}(=\text{O})^\bullet$ and $\text{HC}(=\text{O})^\bullet$ radicals to alkenes, at the CCSD(T)/aug-cc-pVDZ//BHandHLYP/6-311G** level, indicates that both radicals display ambiphilic behaviour. For the $\text{HC}(=\text{O})^\bullet$ radical this behaviour occurs because a secondary orbital interaction of the type $\pi^*_{\text{C=O}} \leftarrow \text{HOMO}$ acts in conjunction with the primary $\text{SOMO} \leftarrow \text{HOMO}$ interaction to balance the $\text{SOMO} \rightarrow \text{LUMO}$ interaction. For the $\text{H}_2\text{P}(=\text{O})^\bullet$ radical, on the other hand, the much higher-lying LUMO (the $\sigma^*_{\text{P-O}}$ orbital) allows for only minimal secondary interaction, and this radical's ambiphilic behaviour is therefore reflective of a balance between $\text{SOMO} \rightarrow \text{LUMO}$ and $\text{SOMO} \leftarrow \text{HOMO}$ interactions.

Introduction

Acyl radicals $\text{RC}(=\text{O})^\bullet$ and their phosphorus analogues, phosphonyl radicals $\text{R}_2\text{P}(=\text{O})^\bullet$ §, are two synthetically valuable classes of reactive intermediates. Acyl radicals, for example, are key components of efficient methods for the construction of carbon–carbon and carbon–nitrogen bonds.¹ While phosphonyl radicals are also employed for direct bond formation, the majority of their current synthetic value lies in their use as alternatives to tin-based reagents for mediating radical chain reactions.²

Acyl radicals had previously been described as nucleophilic in their additions to $\text{C}=\text{C}$ bonds,³ but it was then found that their additions to $\text{C}=\text{N}$ bonds proceeded selectively *via* attack at the electron-rich nitrogen atom.⁴ This surprising selectivity was explored by computational analysis, and was found to result from a strong secondary orbital interaction between the nitrogen lone pair and the acyl π^* orbital.⁵ It is now understood that a combination of orbital interactions— $\alpha\text{-SOMO} \rightarrow \text{LUMO}$, $\beta\text{-SOMO} \leftarrow \text{HOMO}$, and $\pi^* \leftarrow \text{HOMO}$ —contributes to the selectivities of these and related radicals.⁶

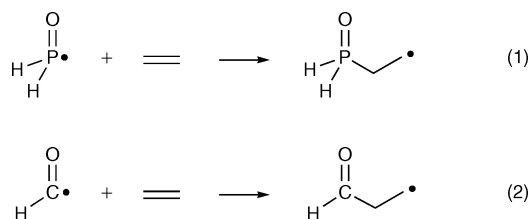
The additions of phosphonyl radicals to $\text{C}=\text{C}$ bonds, by contrast, appear to show no obvious selectivity. For example, the following order of rate constants has been reported⁷ for addition of the $\text{Ph}_2\text{P}(=\text{O})^\bullet$ radical to alkenes: vinyl acetate < vinyl butyl ether < acrylonitrile < methyl acrylate < methacrylonitrile < styrene < methyl methacrylate. The rate constants in the above series vary only from 1.6×10^6 to 8.0×10^7 $\text{L mol}^{-1} \text{s}^{-1}$ (room temperature).

We wondered whether the minimal substrate preferences observed for phosphonyl radicals could be described through simple frontier-orbital considerations (the $\alpha\text{-SOMO} \rightarrow \text{LUMO}$ and $\beta\text{-SOMO} \leftarrow \text{HOMO}$ interactions), or if they are instead a reflection of multi-component orbital interactions like those discovered for their acyl counterparts ($\text{LUMO} \leftarrow \text{HOMO}$). To answer this question, we here examine the additions of the parent radicals $\text{H}_2\text{P}(=\text{O})^\bullet$ and $\text{HC}(=\text{O})^\bullet$ to various unsaturated derivatives, and undertake an examination of the key orbital interactions taking place in each case.

Results and discussion

Choice of computational methods

In order to identify an appropriate computational approach, we first compared the performance of various theoretical methods by calculating the barriers for addition to ethylene (Scheme 1). Data from this assessment are portrayed schematically in Fig. 1.



Scheme 1

^aAustralian Research Council Centre of Excellence for Free Radical Chemistry and Biotechnology, Australia

^bResearch School of Chemistry, The Australian National University, Canberra ACT 0200, Australia

^cSchool of Chemistry, The University of Melbourne, Victoria, Australia 3010

^dBio21 Molecular Science and Biotechnology Institute, The University of Melbourne, Victoria, Australia 3010

† Electronic supplementary information (ESI) available: BHandHLYP/6-311G** geometries of all reactants, complexes, transition states, and products, and total-energy data associated with the assessment of computational methods. See DOI: 10.1039/b714597g

‡ Current address: Department of Chemistry and Biochemistry, University of California, Los Angeles, California 90095, USA. E-mail: krenske@chem.ucla.edu

§ The correct IUPAC designation for radicals of the type $\text{R}_2\text{P}(=\text{O})^\bullet$ is “phosphinoyl”, as they are formally derived from phosphinic acid $\text{H}_2\text{P}(=\text{O})(\text{OH})$. For example, $(\text{CH}_3)_2\text{P}(=\text{O})^\bullet$ is the “dimethylphosphinoyl” radical. In this article, however, we have adopted the common practice of referring to the radicals as “phosphonyl” radicals.

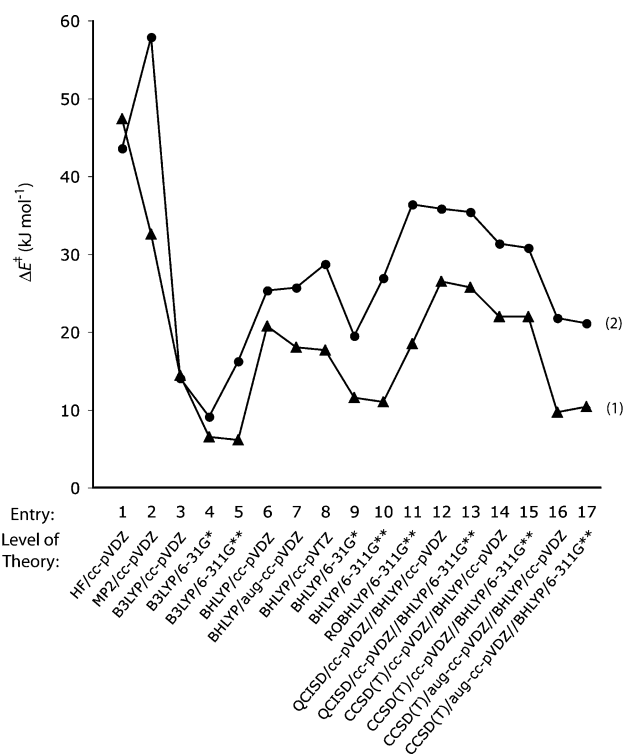


Fig. 1 Energy barriers (ΔE^\ddagger) calculated at various levels of theory for addition of the $\text{H}_2\text{P}(=\text{O})^\bullet$ (1) and $\text{HC}(=\text{O})^\bullet$ (2) radicals to ethylene. Barriers are calculated with respect to the separated reactants. Calculations use an unrestricted representation for open-shell species unless otherwise indicated.

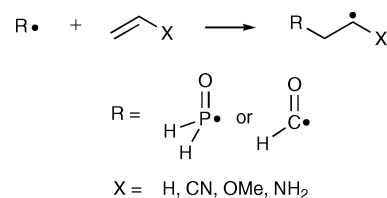
Amongst the various low-cost procedures investigated, the MP2/cc-pVDZ method is noteworthy in providing high estimates of the barriers. B3LYP-based approaches give low estimates, even when a small basis set is employed. These deficiencies have previously been observed for similar reactions of the $\text{CH}_3\text{C}(=\text{O})^\bullet$ radical.⁵ By contrast, calculations using the BHandHLYP functional provide pleasing agreement with the highest levels of theory tested. When improved energies are calculated from BHandHLYP structures by means of single-point calculations, there is the expected progression towards lower barriers as better treatments of correlation and a larger basis set are introduced (*i.e.* from entries 12–13 to entries 14–15 to entries 16–17). The choice of basis set (cc-pVDZ or 6-311G**) used for the initial optimisation appears to make little difference to the barriers obtained *via* QCISD or CCSD(T) single-point calculations. However, the barriers obtained at the BHandHLYP/6-311G** level show much better agreement with the higher-level data than do those obtained at the BHandHLYP/cc-pVDZ level. It would appear that the BHandHLYP/6-31G* and BHandHLYP/6-311G** levels of theory provide reasonable approximations to the higher-level barriers.

For our analysis, we have chosen to employ the CCSD(T)/aug-cc-pVDZ//BHandHLYP/6-311G** level of theory. For one of the test reactions—reaction (2)—the performance of this level of theory can be compared with previously-reported experimental gas-phase kinetic data:⁸ from the reported value for E_a of 23 kJ mol⁻¹ at 298 K, one obtains a value for ΔH^\ddagger_{298} of 21 kJ mol⁻¹. The calculated value of ΔH^\ddagger_{298} at the CCSD(T)/aug-cc-pVDZ//BHandHLYP/6-

311G** level, ignoring the effect of any pre-complexation, is 25 kJ mol⁻¹.

Kinetics and thermodynamics of additions to unsaturated substrates

To compare the reactivities of the $\text{H}_2\text{P}(=\text{O})^\bullet$ and $\text{HC}(=\text{O})^\bullet$ radicals towards C=C bonds, we examined the additions depicted in Scheme 2. Most of these additions proceed through an initial van der Waals complex prior to formation of the transition state. The geometries of the transition states are shown in Fig. 2, and the calculated thermodynamic and kinetic parameters are presented in Table 1.



Scheme 2

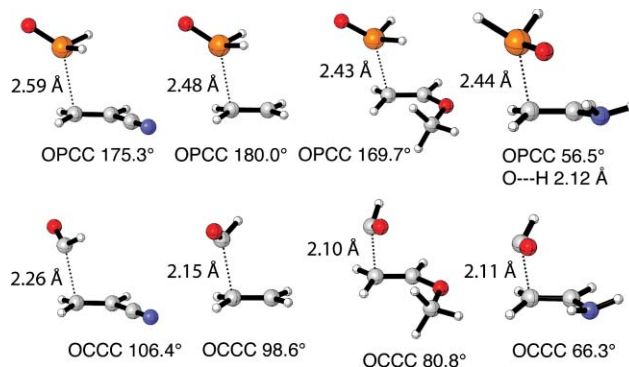


Fig. 2 Transition structures for addition of the $\text{H}_2\text{P}(=\text{O})^\bullet$ and $\text{HC}(=\text{O})^\bullet$ radicals to the alkenes $\text{CH}_2=\text{CH}(\text{CN})$, $\text{CH}_2=\text{CH}_2$, $\text{CH}_2=\text{CH}(\text{OMe})$, and $\text{CH}_2=\text{CH}(\text{NH}_2)$. The forming bond lengths and the dihedral angles about the forming bond are shown.

For both radicals, addition to the alkenes is exothermic. The values of ΔE largely mirror the abilities of the substituent X to stabilise the product radical. In keeping with the normal strengths of P–C and C–C bonds, addition of the $\text{H}_2\text{P}(=\text{O})^\bullet$ radical to a given alkene is *ca.* 30 kJ mol⁻¹ less exothermic than addition of the $\text{HC}(=\text{O})^\bullet$ radical.

Despite their lower thermodynamic driving force, the additions of the $\text{H}_2\text{P}(=\text{O})^\bullet$ radical have lower barriers than those of the $\text{HC}(=\text{O})^\bullet$ radical. This is true whether the barriers are calculated with respect to the van der Waals complexes or to the separated reactants. The higher reactivity of the phosphonyl radical is consistent with experimental precedent: for example, while the $\text{Ph}_2\text{P}(=\text{O})^\bullet$ radical reacts with acrylonitrile with a rate constant of 2.0×10^7 L mol⁻¹ s⁻¹ (room temperature),⁷ the $^t\text{BuC}(=\text{O})^\bullet$ radical adds to the same substrate with a rate constant of 5×10^5 L mol⁻¹ s⁻¹ (300 K)³⁶ and the $^n\text{PrC}(=\text{O})^\bullet$ radical adds to ethylene with a rate constant of 1.4×10^3 L mol⁻¹ s⁻¹ (453 K).⁹

Table 1 Kinetic and thermodynamic parameters for additions of the $\text{H}_2\text{P}(=\text{O})^\bullet$ and $\text{HC}(=\text{O})^\bullet$ radicals to alkenes^a

	ΔE Complex formation	ΔE^\ddagger From reactants	ΔE^\ddagger From complex	ΔE Overall	
$\text{H}_2\text{P}(=\text{O})^\bullet$ plus	$\text{CH}_2=\text{CH}(\text{CN})$	-11.1	8.4	19.5	-76.3
	$\text{CH}_2=\text{CH}_2$	-14.5	10.4	24.9	-58.0
	$\text{CH}_2=\text{CH}(\text{OMe})$	-10.9	6.5	17.4	-62.2
	$\text{CH}_2=\text{CH}(\text{NH}_2)$ (H-bonded TS)	-24.7	-8.7	15.9	-81.1
	$\text{CH}_2=\text{CH}(\text{NH}_2)$ (no H-bond in TS) ^b	-22.5	-3.1	19.3	-81.1
$\text{HC}(=\text{O})^\bullet$ plus	$\text{CH}_2=\text{CH}(\text{CN})$	— ^c	12.6	— ^c	-112.4
	$\text{CH}_2=\text{CH}_2$	-8.2	21.1	29.3	-87.1
	$\text{CH}_2=\text{CH}(\text{OMe})$	-13.7	15.5	29.3	-91.1
	$\text{CH}_2=\text{CH}(\text{NH}_2)$	-16.8	0.3	17.1	-105.0

^a Values (kJ mol^{-1}) calculated at the CCSD(T)/aug-cc-pVDZ//BHandHLYP/6-311G** level of theory. ^b Alternative conformation of transition state in which $\text{H}_2\text{P}(=\text{O})$ unit was rotated so as to prevent $\text{O}\cdots\text{H}-\text{N}$ interaction. ^c No complex found.

Taking addition to ethylene as a reference system, one finds that both radicals experience lower barriers if either an electron-donating substituent (OMe, NH_2) or an electron-withdrawing substituent (CN) is attached to the double bond. That is, both radicals display ambiphilic behaviour, with the changeover point from apparently nucleophilic behaviour to apparently electrophilic behaviour occurring roughly at the parent system (within the sample of alkenes examined).

The ambiphilic behaviour of the $\text{HC}(=\text{O})^\bullet$ radical is surprising in view of the reported nucleophilic tendencies of acyl radicals towards alkenes.³ Conventionally, a nucleophilic radical may be defined¹⁰ as one for which (with a given substrate) the $\alpha\text{-SOMO}\rightarrow\text{LUMO}$ interaction is stronger than the $\beta\text{-SOMO}\leftarrow\text{HOMO}$ interaction. For an electrophilic radical the reverse is true. An ambiphilic radical is then one in which the two interactions are of similar magnitude. However, for a radical such as $\text{HC}(=\text{O})^\bullet$, secondary back-donation into the $\text{C}=\text{O}$ π^* orbital can act together with the $\beta\text{-SOMO}\leftarrow\text{HOMO}$ interaction to yield a more facile reaction when the substrate is sufficiently electron-rich.

The generally lower barriers for the $\text{H}_2\text{P}(=\text{O})^\bullet$ radical allow for less absolute variation in barrier heights as the electronic properties of the alkene are altered. However, in a *relative* sense, when comparing the substrates ethylene and acrylonitrile, the $\text{H}_2\text{P}(=\text{O})^\bullet$ radical appears to respond less dramatically to the decrease in alkene electron density than does the $\text{HC}(=\text{O})^\bullet$ radical. That is, on going from ethylene to acrylonitrile, the barrier for $\text{H}_2\text{P}(=\text{O})^\bullet$ decreases from 10.4 to 8.4 kJ mol^{-1} , compared with a decrease from 21.1 to 12.6 kJ mol^{-1} for $\text{HC}(=\text{O})^\bullet$. By contrast, on going from ethylene to the more electron-rich alkenes, the radicals' relative responses are not so markedly divergent.

Orbital interactions

In order to ascertain whether the ambiphilic behaviour of the $\text{H}_2\text{P}(=\text{O})^\bullet$ radical reflects a contribution from secondary back-donation, we have sought recourse to a variety of theoretical models.

Frontier orbital analysis. Simple frontier orbital considerations suggest that both the $\text{H}_2\text{P}(=\text{O})^\bullet$ and $\text{HC}(=\text{O})^\bullet$ radicals should be somewhat ambiphilic towards alkenes. A diagram

showing the frontier orbital energies of the two radicals and their four substrates is given in Fig. 3. From the figure it appears that the filled $\alpha\text{-SOMO}$ and unfilled $\beta\text{-SOMO}$ of both radicals are roughly equally matched with their partner orbitals in the alkene (the LUMO and HOMO, respectively), with a slight leaning towards the electrophilic $\beta\text{-SOMO}\text{-HOMO}$ pairing. While this prediction is only approximate, one may note that the lower $\alpha\text{-SOMO}$ energy of $\text{H}_2\text{P}(=\text{O})^\bullet$ would suggest a lower nucleophilicity for this radical. This would lead to a smaller variation in interaction when the alkene LUMO energy is lowered, which agrees with the finding that the $\text{H}_2\text{P}(=\text{O})^\bullet$ radical responds less dramatically to the decrease in alkene electron-density on going from ethylene to acrylonitrile than does the $\text{HC}(=\text{O})^\bullet$ radical.

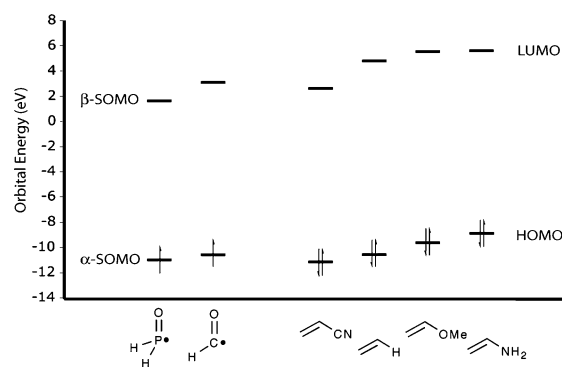


Fig. 3 Orbital energies for the $\text{H}_2\text{P}(=\text{O})^\bullet$ and $\text{HC}(=\text{O})^\bullet$ radicals and the alkenes $\text{CH}_2=\text{CH}(\text{CN})$, $\text{CH}_2=\text{CH}_2$, $\text{CH}_2=\text{CH}(\text{OMe})$, and $\text{CH}_2=\text{CH}(\text{NH}_2)$, calculated at the HF/6-31G(d) level of theory.

Transition state geometries. It has previously been noted that the secondary $\pi^*_{\text{C}=\text{O}}\leftarrow\text{HOMO}$ interaction for acyl radicals is reflected in unusual transition state geometries.^{1,5} As shown in Fig. 4(a), the SOMO and π^* orbital of the $\text{HC}(=\text{O})^\bullet$ radical are perpendicular to each other; therefore, to accommodate both the primary and the secondary interactions, the HCO plane must tilt towards the alkene and the $\text{C}=\text{O}$ unit must rotate towards the $\text{C}=\text{C}$ bond. These features are evident in the transition state geometries that were shown in Fig. 2.

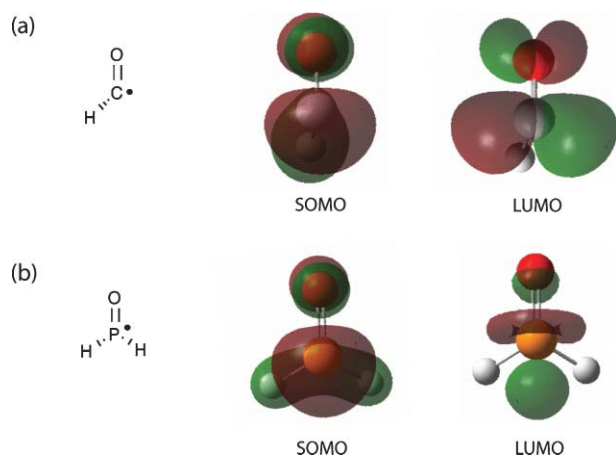


Fig. 4 Orbitals of the $\text{H}_2\text{P}(=\text{O})^\bullet$ and $\text{HC}(=\text{O})^\bullet$ radicals, calculated at the UBHandHLYP/6-311G** level of theory (α orbitals shown). Surfaces are drawn at an isodensity value of 0.06.

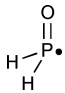
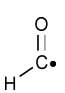
For the $\text{H}_2\text{P}(=\text{O})^\bullet$ radical, by contrast, geometrical features do not reveal whether a secondary orbital interaction is significant. Because the LUMO of the $\text{H}_2\text{P}(=\text{O})^\bullet$ radical is cylindrically symmetrical about the P–O axis and occupies the same plane as the SOMO [Fig. 4(b)], it can (in principle) interact with the substrate HOMO without requiring a substantial reorientation of radical and substrate.

We should point out that the transition structure for addition of the $\text{H}_2\text{P}(=\text{O})^\bullet$ radical to $\text{CH}_2=\text{CH}(\text{NH}_2)$ does not resemble the others. Here, a hydrogen-bonding interaction between the phosphoryl oxygen and the amine hydrogen results in a different orientation of the radical with respect to the substrate. This hydrogen-bonding interaction is partly responsible for the low barrier seen in this reaction. If the phosphoryl radical is rotated so that the P=O and C=C bonds are staggered, the barrier increases by approximately 4 kJ mol⁻¹ (although still remaining the lowest of the series when calculated with respect to the reactants).

Theoretical reactivity predictors. Two quantities that influence potential orbital interactions are the radicals' vertical ionisation potentials and electron affinities. Calculated values for these quantities are shown in Table 2.

Taken together, the data in Table 2 indicate the $\text{H}_2\text{P}(=\text{O})^\bullet$ radical to have substantially greater oxidising power than the $\text{HC}(=\text{O})^\bullet$ radical. One may calculate that it has both a higher electronegativity [defined as $(\text{IP} + \text{EA})/2$] and a lower chemical

Table 2 Vertical ionisation potentials and electron affinities of the $\text{H}_2\text{P}(=\text{O})^\bullet$ and $\text{HC}(=\text{O})^\bullet$ radicals^a

		
IP	9.5	9.0
EA	1.2	-0.4

^a Values (eV) calculated at the CCSD(T)/aug-cc-pVDZ//BHandHLYP/6-311G** level.

hardness [defined as $(\text{IP} - \text{EA})/2$]; these features favour electron-transfer to the SOMO and suggest enhanced electrophilic-radical character.

Natural bond orbital analysis. Natural bond orbital (NBO) analysis has previously proven useful for uncovering the importance of the $\pi^*_{\text{C=O}} \leftarrow \text{HOMO}$ secondary orbital interaction relative to the primary $\alpha\text{-SOMO} \rightarrow \text{LUMO}$ interaction during the addition reactions of acyl radicals.^{1,5} We have likewise calculated the NBO donor–acceptor interaction energies in the transition states for addition of the $\text{H}_2\text{P}(=\text{O})^\bullet$ and $\text{HC}(=\text{O})^\bullet$ radicals to the four alkenes. The relevant data are shown in Table 3. In this table, only interactions within the α spin set are shown. That is, the interactions being shown are the α (nucleophilic) component of the “primary interaction” (*i.e.* $\alpha\text{-SOMO} \rightarrow \text{LUMO}$) and the α component of the “secondary interaction” ($\alpha\text{-LUMO} \leftarrow \text{HOMO}$ back-donation). The $\beta\text{-SOMO} \leftarrow \text{HOMO}$ interaction, which is the electrophilic component of the “primary interaction”, could not be measured.¹¹

As expected, the $\text{HC}(=\text{O})^\bullet$ radical undergoes a strong secondary orbital interaction during addition to the electron-rich alkenes $\text{CH}_2=\text{CH}(\text{NH}_2)$ and $\text{CH}_2=\text{CH}(\text{OMe})$. In its most pronounced case, the secondary interaction (74 kJ mol⁻¹) has a value almost equal to that of the primary $\text{SOMO} \rightarrow \text{LUMO}$ interaction (81 kJ mol⁻¹). This is a considerably greater secondary contribution than was previously found for the addition of the $\text{CH}_3\text{C}(=\text{O})^\bullet$ radical to $\text{CH}_2=\text{CH}(\text{NH}_2)$: the corresponding values in that case were 14 and 144 kJ mol⁻¹, respectively.¹²

Contrastingly, the $\text{H}_2\text{P}(=\text{O})^\bullet$ radical is much less prone than either the $\text{HC}(=\text{O})^\bullet$ or the $\text{CH}_3\text{C}(=\text{O})^\bullet$ radical to back-donation. The secondary interaction seen for this radical with any of the alkenes only amounts to a few kJ mol⁻¹.

This dissimilarity is a result of the different electronic structures of the P=O and C=O bonds. It is well known¹³ that the P=O bond in phosphorus(V) species is most appropriately denoted not by a traditional $\sigma + \pi$ structure but by a σ bond and an additional electrostatic attraction, *i.e.* $\text{P}^+ - \text{O}^-$. Accordingly, the LUMO of the $\text{H}_2\text{P}(=\text{O})^\bullet$ radical is a P–O σ^* orbital. Because the energy gap between the SOMO and the P–O σ^* orbital of the $\text{H}_2\text{P}(=\text{O})^\bullet$ radical is some 1.5 eV wider than the gap between the SOMO and the C=O π^* orbital of the $\text{HC}(=\text{O})^\bullet$ radical (at the BHandHLYP/6-311G** level), the ability of the $\text{H}_2\text{P}(=\text{O})^\bullet$ radical to accept electron density *via* secondary back-donation is much lower.

The alkenes in Table 3 are relatively weak donors, and to gain an indication of the possible magnitude of a $\sigma^*_{\text{P-O}} \leftarrow \text{HOMO}$ interaction we therefore also considered addition to the electron-rich nitrogen atom of $\text{CH}_2=\text{NH}$. The NBO data for these reactions are included in Table 3. Thus, with $\text{CH}_2=\text{NH}$, the $\sigma^*_{\text{P-O}} \leftarrow \text{lone-pair}$ interaction provides a contribution of 16 kJ mol⁻¹. While not insignificant, this value is modest in comparison to the $\pi^*_{\text{C=O}} \leftarrow \text{lone-pair}$ interaction for the $\text{HC}(=\text{O})^\bullet$ radical, which amounts to 205 kJ mol⁻¹.

Concluding remarks

Our calculations demonstrate the $\text{H}_2\text{P}(=\text{O})^\bullet$ and $\text{HC}(=\text{O})^\bullet$ radicals to have similar overall reactivity trends towards alkenes, but these trends stem from different orbital contributions. The

Table 3 Major NBO interactions occurring in the α spin set in the transition states for additions of the $\text{H}_2\text{P}(=\text{O})^\bullet$ and $\text{HC}(=\text{O})^\bullet$ radicals to $\text{C}=\text{C}$ and $\text{C}=\text{N}$ bonds^a

Substrate	Primary interaction SOMO \rightarrow π^*	Secondary interaction LUMO \leftarrow π	Primary interaction SOMO \rightarrow π^*	Secondary interaction LUMO \leftarrow π	Primary interaction SOMO \rightarrow π^*	Secondary interaction LUMO \leftarrow π
$\text{CH}_2=\text{CH}(\text{CN})$	107	2	137	2	137	7
$\text{CH}_2=\text{CH}_2$	140	4	163	4	163	9
$\text{CH}_2=\text{CH}(\text{OMe})$	148	4	159	4	159	29
$\text{CH}_2=\text{CH}(\text{NH}_2)^b$	77	1	81	1	81	74
$\text{CH}_2=\text{NH}$ (<i>via</i> N)	161	0.6	22	16	22	205

^a Interaction energies (kJ mol^{-1}) calculated at the BHandHLYP/6-311G** level from the α donor-acceptor interactions calculated by second-order perturbation theory analysis on the calculated NBOs, using a constrained Lewis structure, as described in the text. ^b No hydrogen-bond in the transition state for the $\text{H}_2\text{P}(=\text{O})^\bullet$ radical.



limited capacity for back-donation of the type $\sigma_{\text{P-O}}^* \leftarrow \text{HOMO}$ (revealed by NBO analysis) and the enhanced capacity for charge-transfer to the β -SOMO (calculated from IP and EA data) indicate the $\text{H}_2\text{P}(=\text{O})^\bullet$ radical to rely predominantly on conventional α -SOMO \rightarrow LUMO and β -SOMO \leftarrow HOMO interactions. Although this radical displays a much higher reactivity towards $\text{C}=\text{C}$ bonds than does its carbon counterpart, such reactivity appears not to be problematic in synthetic contexts: that is, unwanted addition of phosphoryl radicals to double bonds has only rarely been reported to affect their synthetic use as chain carriers,² and they serve as valuable agents for mediating radical transformations.

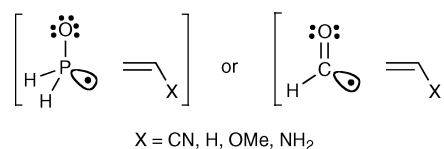
Computational details

Standard *ab initio* molecular orbital theory¹⁴ and density functional theory (DFT)¹⁵ calculations were carried out using GAUSSIAN 03.¹⁶ Unless otherwise indicated, calculations on open-shell species were performed with an unrestricted wavefunction.

The performance of various *ab initio* and DFT methods was assessed through calculation of the barriers for addition of the $\text{H}_2\text{P}(=\text{O})^\bullet$ and $\text{HC}(=\text{O})^\bullet$ radicals to ethylene. During this assessment, full conformational searching was performed for each level of theory at which geometrical optimisation was conducted. Total energies and the resulting barriers are provided in the ESI†.

Subsequently, the geometries of all reactants, complexes, transition states, and products were optimised at the BHandHLYP/6-311G** level of theory. Thorough conformational searching was again performed so as to identify the global minimum-energy conformer of each species. The BHandHLYP/6-311G** vibrational frequencies were used to confirm the nature of each stationary point, and to calculate (unscaled) zero-point energies and temperature corrections to the enthalpies, where appropriate. For each transition structure, an intrinsic reaction coordinate (IRC) calculation¹⁷ was carried out at the BHandHLYP/6-311G** level, in order to verify that the geometry represented the correct first-order saddle point on the surface connecting reactants to product. Improved energies for all species were then obtained *via* single-point calculations at the CCSD(T)/aug-cc-pVDZ level. Optimised geometries at the BHandHLYP/6-311G** level, in the form of Gaussian archive entries, are provided in the ESI†.

Natural bond orbital (NBO) analyses¹⁸ were performed at the BHandHLYP/6-311G** level. So as to avoid the treatment of the transition states as bound units, the Lewis structures were explicitly constrained to a two-unit structure using the most chemically reasonable representation of each attacking radical, as shown in Scheme 3. This provided a qualitatively acceptable representation of the orbitals corresponding to the radical α -SOMO and the alkene π and π^* orbitals. Due to the non-correspondence of the β orbitals,¹¹ only the α spin set was used to derive interaction data.



Scheme 3

Acknowledgements

We acknowledge the financial support of the Australian Research Council's Centres of Excellence Program. Generous amounts of computer time were made available by the Australian Partnership for Advanced Computing, the Australian National University Supercomputer Facility, and the University of California, Los Angeles. Helpful discussion with Professor Kendall Houk is gratefully acknowledged.

Notes and references

- 1 Review: C. H. Schiesser, U. Wille, H. Matsubara and I. Ryu, *Acc. Chem. Res.*, 2007, **40**, 303–313.
- 2 D. H. R. Barton, D. O. Jang and J. C. Jaszberenyi, *J. Org. Chem.*, 1993, **58**, 6838–6842.
- 3 (a) C. Chatgililoglu, D. Crich, M. Komatsu and I. Ryu, *Chem. Rev.*, 1999, **99**, 1991–2069; (b) F. Jent, H. Paul, E. Roduner, M. Heming and H. Fischer, *Int. J. Chem. Kinet.*, 1986, **18**, 1113–1122.
- 4 I. Ryu, K. Matsu, S. Minakata and M. Komatsu, *J. Am. Chem. Soc.*, 1998, **120**, 5838–5839; M. Tojino, N. Otsuka, T. Fukuyama, H. Matsubara, C. H. Schiesser, H. Kuriyama, H. Miyazato, S. Minakata, M. Komatsu and I. Ryu, *Org. Biomol. Chem.*, 2003, **1**, 4262–4267; I. Ryu, H. Miyazato, H. Kuriyama, K. Matsu, M. Tojino, T. Fukuyama, S. Minakata and M. Komatsu, *J. Am. Chem. Soc.*, 2003, **125**, 5632–5633.
- 5 C. T. Falzon, I. Ryu and C. H. Schiesser, *Chem. Commun.*, 2002, 2338–2339; C. H. Schiesser, H. Matsubara, I. Ritsner and U. Wille, *Chem. Commun.*, 2006, 1067–1069; H. Matsubara, C. T. Falzon, I. Ryu and C. H. Schiesser, *Org. Biomol. Chem.*, 2006, **4**, 1920–1926.
- 6 S. H. Kyne, C. H. Schiesser and H. Matsubara, *Org. Biomol. Chem.*, 2007, **5**, 3938–3943.
- 7 T. Sumiyoshi and W. Schnabel, *Makromol. Chem.*, 1985, **186**, 1811–1823.
- 8 R. Lesclaux, P. Roussel, B. Veyret and C. Pouchan, *J. Am. Chem. Soc.*, 1986, **108**, 3872–3879.
- 9 A. G. Shostenko, P. A. Zagorets, N. P. Tarasova and V. E. Myshkin, *J. Radioanal. Chem.*, 1979, **51**, 337–344.
- 10 J. Fossey, D. Lefort and J. Sorba, *Free Radicals in Organic Chemistry*, Wiley, Chichester, 1995, ch. 6.
- 11 During NBO analysis of the $\text{H}_2\text{P}(=\text{O})^\bullet$ and $\text{HC}(=\text{O})^\bullet$ radicals, the presence of additional non- σ electrons in the vicinity of the radical centre led to a mismatch of orbital representations in the α and β spin sets, such that no valence β orbital (corresponding to the β -SOMO) was located on the radical centre. Constraint of the radicals' resonance structures to the most suitable canonical contributor was not sufficient to overcome this effect. Therefore, we only cite data for the α interactions. The results in Table 3 indicate the relative magnitudes of the α (nucleophilic) component of the primary interaction and the α component of the secondary backdonation, without considering the β (electrophilic) component of the primary interaction or the β secondary interaction.
- 12 C. H. Schiesser and S. H. Kyne, unpublished work.
- 13 L. D. Quin, *A Guide to Organophosphorus Chemistry*, Wiley-Interscience, New York, 2000, ch. 1, pp. 12–15.
- 14 W. J. Hehre, L. Radom, P. v. R. Schleyer and J. A. Pople, *Ab Initio Molecular Orbital Theory*, Wiley, New York, 1986.
- 15 W. Koch and M. C. Holthausen, *A Chemist's Guide to Density Functional Theory*, Wiley-VCH, Weinheim, 2000.
- 16 M. J. Frisch, G. W. Trucks, H. B. Schlegel, G. E. Scuseria, M. A. Robb, J. R. Cheeseman, J. A. Montgomery, Jr., T. Vreven, K. N. Kudin, J. C. Burant, J. M. Millam, S. S. Iyengar, J. Tomasi, V. Barone, B. Mennucci, M. Cossi, G. Scalmani, N. Rega, G. A. Petersson, H. Nakatsuji, M. Hada, M. Ehara, K. Toyota, R. Fukuda, J. Hasegawa, M. Ishida, T. Nakajima, Y. Honda, O. Kitao, H. Nakai, M. Klene, X. Li, J. E. Knox, H. P. Hratchian, J. B. Cross, V. Bakken, C. Adamo, J. Jaramillo, R. Gomperts, R. E. Stratmann, O. Yazyev, A. J. Austin, R. Cammi, C. Pomelli, J. W. Ochterski, P. Y. Ayala, K. Morokuma, G. A. Voth, P. Salvador, J. J. Dannenberg, V. G. Zakrzewski, S. Dapprich, A. D. Daniels, M. C. Strain, O. Farkas, D. K. Malick, A. D. Rabuck, K. Raghavachari, J. B. Foresman, J. V. Ortiz, Q. Cui, A. G. Baboul, S. Clifford, J. Cioslowski, B. B. Stefanov, G. Liu, A. Liashenko, P. Piskorz, I. Komaromi, R. L. Martin, D. J. Fox, T. Keith, M. A. Al-Laham, C. Y. Peng, A. Nanayakkara, M. Challacombe, P. M. W. Gill, B. Johnson, W. Chen, M. W. Wong, C. Gonzalez and J. A. Pople, *Gaussian 03, Revision C.02*, Gaussian, Inc., Wallingford CT, 2004.
- 17 C. Gonzalez and H. B. Schlegel, *J. Chem. Phys.*, 1989, **90**, 2154–2161.
- 18 E. D. Glendening, A. E. Reed, J. E. Carpenter and F. Weinhold, *NBO Version 3.1*.